Available online at www.sciencedirect.com

ScienceDirect

Scripta Materialia 102 (2015) 27–30

Scripta MATERIALIA

www.elsevier.com/locate/scriptamat

Crystal size effect in two dimensions – Influence of size and shape

R. Maaß,[a,*] C.A. Volkert[a] and P.M. Derlet[b]

[a]*Institute for Materials Physics, University of Göttingen, Friedrich-HundPlatz 1, 37077 Göttingen, Germany*
[b]*Paul Scherrer Institut, Condensed Matter Theory, 5232 Villigen PSI, Switzerland*

Received 1 January 2015; revised 30 January 2015; accepted 1 February 2015
Available online 19 February 2015

Based on the statistics of both the stress and strain of a plastic event, the well known size-effect in strength can be linked to a crystal's critical stress distribution and the universal scaling exponent of intermittent plasticity. We successfully test these hypotheses with small-scale deformation experiments as a function of diameter and aspect ratio, and find that the latter affects the material's strength in a way that gives direct insight into the underlying critical stress distribution of the deforming volume.

Keywords: Size effect; Plasticity; Single crystals; Stress scaling

Classical laws on strength of crystalline materials did consider strength to be independent of external dimensions of the tested material. About 10 years ago it was convincingly demonstrated that there is an extrinsic size-strength scaling in crystal plasticity at small scales that is well described by a power-law: $\sigma \propto d^{-n}$, where σ is the flow strength and d is some measure of crystal size. Today's consolidated picture of this strength-size scaling shows that n is strongly dependent on the initial microstructure of the material [1–3].

While no size-scaling exists at the macroscopic scale, bulk crystals have in common with their small counterparts that their elastic to plastic transition is also very much dependent on the details of the underlying microstructure. More specifically, it is the initial defect structure that determines strength across all length scales. The mobile part of the dislocation network will facilitate plastic deformation by collectively moving and multiplying within the crystal. Such plastic activity – may it be in a bulk or small-scale crystal – can be characterized by the external stress at which it occurs and thus the statistical properties of the early stages of a deformation sequence should be strongly influenced by a distribution $P(\sigma_c)$ of such critical stresses. $P(\sigma_c)$ therefore characterizes the underlying dislocation network microstructure in terms of the stress scale at which plastic evolution occurs.

In addition to the strength determining initial defect distribution, crystals at all length scales deform plastically in a discrete fashion in terms of both stress and plastic strain [4]. At the bulk scale this is hard to observe in a regular straining experiment, with the exception of some cases of ultra high strain resolution [5]. Reducing sample size, the intermittency of the discretely evolving dislocation structure can be readily observed with nano-scale extensometry, which reinvigorated numerous efforts investigating scale-free slip events [6,7] as well as the temporal dynamics of avalanches [8,9] occurring in critically evolving dislocation systems. The general conclusion became that a plastically evolving dislocation structure exhibits power-law slip-size (plastic strain) distributions, $P(S) \propto S^{-\tau}$, where τ is a critical exponent, suggesting that dislocation based plasticity belongs to a class of phenomenon that is fundamentally scale free and universal [4,10].

Such universality in the statistics of plastic strain implies an insensitivity to the microscopic details, while on the other hand the stress scale at which such plastic events occur does appear to be very dependent on the microstructural details. The emerging questions are how these two very different aspects of deformation can be linked, and how this may result in the "smaller is stronger" paradigm observed in micro-compression experiments? One recent statistical approach which relates these aspects in a unified way gives the simple expression $n = (\tau + 1)/(\alpha + 1)$ [11], for the size-effect exponent, where α is the leading order exponent of the low critical stress side of $P(\sigma_c)$ and τ is the aforementioned critical exponent for scale-free plastic activity. This expression relates material strength (as a function of deforming volume) directly with the universal behavior of intermittent plastic strain activity and the statistics of the critical stresses at which it occurs. As will be subsequently discussed, the developed connection also infers a broader class of scaling laws in which both size and shape can affect material strength. In particular the aspect ratio of a

* Corresponding author; e-mail: robert.maass@ingenieur.de

http://dx.doi.org/10.1016/j.scriptamat.2015.02.006
1359-6462/

micron-sized crystal should affect strength via a scaling law with an exponent equal to $1/(\alpha+1)$. Motivated by these theoretical developments, the present work undertakes an experimental investigation demonstrating that the aspect ratio does indeed affect material strength, and via the above expression it becomes possible to access α and τ from one test series probing crystal size and shape. This combined experimental and theoretical approach links for the first time a universal scaling parameter to simple stress measurements, and indicates that the size-effect in strength partly is universal to crystalline metallic materials.

Cylindrical nano- and micro-crystals with a compression axis along the ⟨001⟩-axis were prepared by focused ion beam milling from a single crystal (Mateck). The specimens were compressed at a nominal strain rate of $5\times10^{-3}\,s^{-1}$ inside a Hysitron Nanoindenter or in an Agilent G200 Nanoindenter using the DCM module at a nominal force rate of $1.0\,\mu N\,s^{-1}$. The obtained data were converted to engineering stress–strain data, and the flow stress at a plastic strain of 3% was used to construct Figures. 1a, 2a and 3a.

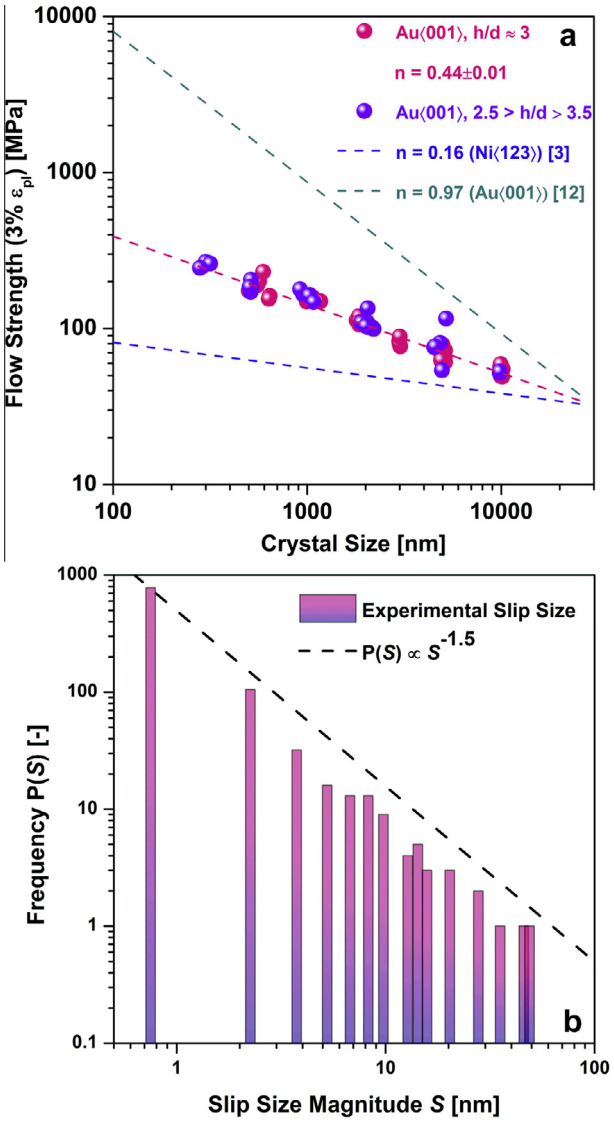

Figure 1. (a) Strength-size scaling for ⟨001⟩-oriented Au crystals, fit to a power-law with a scaling exponent of 0.44. Two different data sets are presented: one with an $A_r = 3$, and one with an $2.5 > A_r > 3.5$. The dashed lines bound the reported experimental limits reported so far. (b) A slip-size distribution obtained from the intermittent slip activity of the deforming Au crystals with $A_r = 3$.

The size-effect model developed in Ref. [11] is based on two distinct size effects – one in stress and one in strain. For the size effect in stress, it is realized that the number of available plastic events, M, should scale linearly with the volume of the deforming material. Sampling the assumed critical stress distribution, $P(\sigma_c)$, M times results in a critical stress sequence whose order statistics is important. Indeed, the characteristic ith smallest critical stress is given by $i = M\int_0^{\langle\sigma_c^i\rangle} P(\sigma)d\sigma$, reflecting the extreme value statistics when M is not small. Thus when the sample volume (and thus M) decreases, the scale of the lowest critical stresses increases. For the case of plastic strain, it was further recognized that under the assumption of self-organized criticality, the magnitude of a plastic strain event is only weakly correlated with the applied stress and that their distribution is truncated by the finite size of the sample. Together this results in an average plastic strain magnitude which scales with volume via the universal critical exponent τ. When combined, the size effects in stress and plastic strain give a simple expression for the stress scaling with respect to system size as (Ref. [11])

$$\sigma \sim \left(\frac{1}{L}\right)^{(1+\tau)/(1+\alpha)}. \tag{1}$$

Here L is a characteristic dimension of the system. For the case of a cylindrical pillar of height h and diameter d, the stress scaling of Eq. (1) is with respect to the minimum external length scale, the pillar diameter ($d = L$) at a *fixed* aspect ratio. Since the critical strain scaling depends only on this minimum external length, changing the pillar height only affects the stress scaling (since it depends on the total sample volume) resulting in an overall stress scaling:

$$\sigma \sim \left(\frac{1}{h}\right)^{\frac{1}{1+\alpha}} \times \left(\frac{1}{d}\right)^{\frac{\tau}{1+\alpha}} = \left(\frac{1}{A_r}\right)^{1/(1+\alpha)} \times \left(\frac{1}{d}\right)^{(1+\tau)/(1+\alpha)}, \tag{2}$$

where in the last equality, the scaling has been written in terms of the aspect ratio $A_r = h/d$. Eq. (2) indicates a dependence on A_r, arising solely from the extreme value statistics of critical stress, thereby providing direct insight into the distribution $P(\sigma_c)$. It is this new aspect of the size-effect in crystal strength which forms the central theme of the present work.

As a first step, the compressive strength at 3% plastic strain of cylindrical gold crystals with diameters ranging between 300 nm and 10 μm is tested and yields the expected trend depicted in Fig. 1a. The very robust scaling for the here studied ⟨001⟩-oriented single crystalline material can be expressed as $\sigma \propto d^{-n}$, with $n = 0.44 \pm 0.1$ ($R^2 = 0.976$, root mean square error (RMSE) = 0.082). This trend includes all investigated aspect ratios and is the essence of many studies of similar sample geometries whose bounds in n are indicated with dashed lines for $n = 0.16$ [3] and ca. 0.9 [12]. For later purposes we display in Fig. 1a the standard $A_r \approx 3$ as one data set and the other A_r covering smaller and larger values in another set. Irrespective of the data sets, all strength values seem to align well with the established power-law scaling and cannot be distinguished from each other.

Before turning our attention to how the data summarized in Fig. 1a can be recast to express scaling with respect

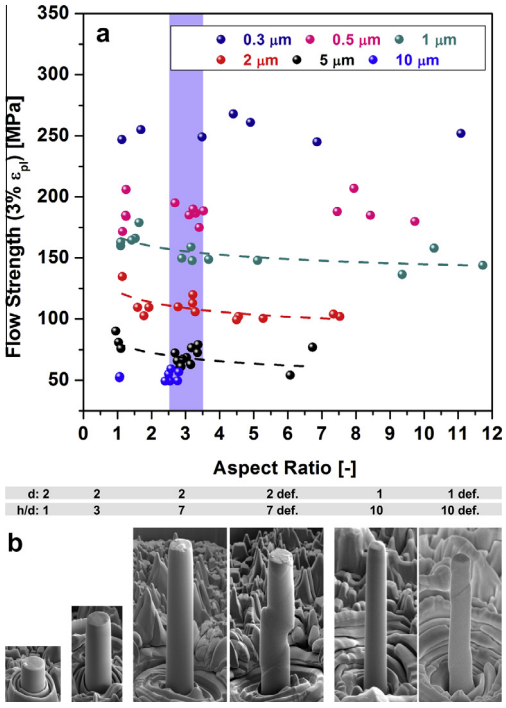

Figure 2. (a) Strength as a function of aspect ratio A_r for different sample sizes. Using Eq. (1), with $\alpha = 4.69$ and $\tau = 1.5$, the dashed lines are obtained, following well the experimental data. A set of samples with different aspect ratios, h/d, is shown in (b).

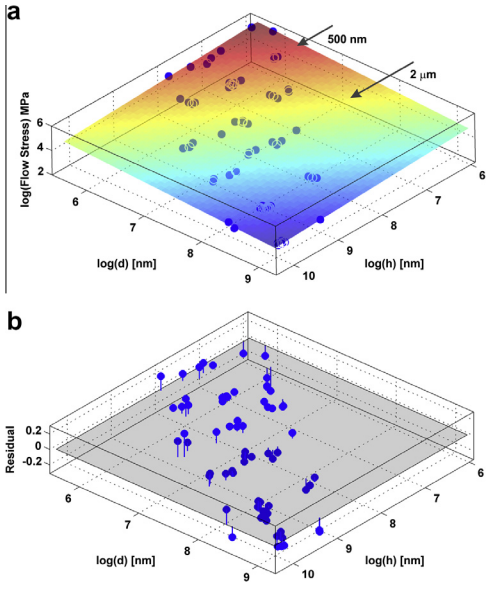

Figure 3. Crystal strength as a function of both cross-sectional diameter d and length h (a), with the plane representing a fit using Eq. (2). The residuals of the fitting between experimental data and Eq. (2) are shown in (b). The arrows in (a) indicate the lines of data for nominally the same diameter of 500 nm and 2 μm.

to size and shape, we show in Fig. 1b the corresponding stress-integrated slip-size distribution, $P(S)$, that was derived following custom methodology based on the thresholding of the displacement–time data's first derivative [9,13]. As expected for universal phenomena and predicted by theoretical mean-field models, the distribution of the stress-integrated slip-size magnitude follows a power-law scaling of type $P(S) \propto S^{-\tau}$ with $\tau \sim 1.5$. Since such a distribution is insensitive to the microscopic details of the dislocation network it should also be insensitive to any initial form of $P(\sigma_c)$. The data of Fig. 1a give a value of $n \sim 0.44$ and of Fig. 1b a value of $\tau \sim 1.5$, which via $n = (\tau + 1)/(\alpha + 1)$ gives $\alpha = 4.69$.

A first step to test the prediction made by Eq. (2) is to verify if there indeed is any strength-scaling with respect to A_r. Therefore we will now sample A_r at a constant crystal size d. The resulting trends for each specimen size are shown in Fig. 2a, and Fig. 2b displays selected un-deformed and deformed crystals imaged with scanning electron microscopy. It is noted that linear scaling is used in Fig. 2a, which greatly enhances the intrinsic scatter of such data that otherwise is routinely summarized in double

logarithmic scaling. Fig. 2a also indicates the regime of $2.5 < h < 3.5$ displayed in Fig. 1a with the shaded background. The strength data in Fig. 2a show a somewhat weak dependence on A_r, which would be expected from the reduced Eq. (2) being a power-law with a scaling exponent of $1/(1+\alpha) = 0.176$, upon setting again $\alpha = 4.69$ and $\tau = 1.5$. This means, the here found strength-shape scaling is of the same order as the lower bound values of the strength-size scaling displayed in Fig. 1a. It is acknowledged that the information content of the accessible data range in Fig. 2a is insufficient to meaningfully fit the full Eq. (2) to the data. It is at this stage only possible to again use the earlier discussed values for both α and τ, and to conclude that the analytical form is compatible with the experimental data, as is indicated for the diameters of 5, 2 and 1 μm. This further leads to the conclusion that tensile experiments will be the ideal means to probe the strength-scaling with respect to A_r, allowing to directly access τ and α.

The next step is to exploit Eq. (2) by constructing a surface plot including both the size d, as well as the height h. This yields the plot displayed in Fig. 3a to which the full analytical model given by Eq. (2) can be fit with the fitting parameters α and using $\tau = 1.5$. Only fitting alpha allows an agreement between model and experiment to a precision of $R^2 = 0.945$, RMSE $= 0.121$, which is of similar quality as the 1D strength data shown in Fig. 1a. It is now quite remarkably seen how the seemingly one dimensional data in Fig. 1a can be broken up to separate between scaling-effects arising due to different dimensions of the crystal. The fitted plane is superimposed with the data in Fig. 3a, and the residuals are shown in Fig. 3b. Data points parallel to the log (h) axis display the different sample diameters as a function of length (exemplarily indicated for 500 nm and 2 μm).

Following this surface fit methodology yields $\alpha = 4.512$ with the 95% confidence bounds being (4.199, 4.824), which is very close to 4.69 as was obtained from the analysis in Fig. 1a. Both these alpha values are not only evidencing a very good agreement between the model developed in Ref. [11], its suggested predictions contained in Eq. (2), and the conducted experiments, but also fall in the range of Weibull parameters $\alpha + 1 = 3.5 - 6.5$ obtained from 2D and 3D discrete dislocation (DD) dynamics simulations, as well as experiments [14,15].

The above analysis and successful demonstration of how the size-effect in strength can be expanded by introducing the aspect ratio as a second scaling variable show that both size and shape can play a role. This experimental finding is in agreement with failure stress dependencies on aspect ratios of three-dimensional spring networks [16,17], as well as 3D-DD simulations [18]. In the former case it was found that the failure stress can be well captured by both Weibull and Gumbel distributions (both also part of the generalized description of the here tested model if the mean of the extreme value statistics is at sufficiently high values such that the negatively valued part of the Gumbel distribution becomes irrelevant [19]) and showed a stress scaling exponent with respect to length at constant base that sensitively depends on the dimensionality and interactions. In the 3D-DD simulations it is found that the flow stress increases with decreasing aspect ratio in ⟨123⟩- and ⟨100⟩-oriented microcrystals. The different behavior of the two crystal orientations was rationalized on the basis of dislocation source statistics on the available glide planes of both orientations. The present work (via Eq. (2)) gives a straight forward origin to these 3D-DD results. Moreover, since the critical stress distribution must ultimately be a function of a stress *tensor*, only becoming a function of a scalar stress measure upon choice of loading geometry, differences in α can be expected for different crystal orientations. Ref. [11] demonstrates that the statistics of flow stress at a fixed plastic strain is well described by a Weibull distribution, even though other distributions are included in the original model of Ref. [11]. Although, Ref. [18] considered a weakest link stress scale scenario for the general size effect, the present model suggests that such a weakest link approach is only applicable to a change in aspect ratio for a fixed pillar diameter. Re-analyzing the data in Fig. 11 of Ref. [18] by considering such data-sets separately gives Weibull moduli ($m = \alpha + 1$) of 3.5, 2.9 and 6.1 for respective diameters of 0.5, 0.75 and 1 micron. In addition, a failure analysis for different plastic evolution realizations gave Weibull distributions with moduli that did not vary too greatly as a function of aspect ratio for a fixed diameter. This suggests an extreme value statistics picture is at play for such DD simulations, and gives values of α that are compatible with the present experimental findings and other DD simulations [20]. While the critical stress sampling, being one of the two main aspects of the here tested model in Ref. [11], seems to be well in line with earlier studies, its connection to the scale-free slip size distribution remains to be experimentally verified. In particular this means to verify if the probed underlying dislocation structure is close enough to criticality in order to exhibit scale free slip-size behavior when the first critical stresses in a sequence are sampled. Another open point is to what degree $\tau = 1.5$ can be assumed to be a fixed value for evolving dislocation networks. Even though there is a vast amount of literature supporting its robustness, recent research points toward deviations from 1.5, reporting a range between 1.0 and 1.9 [20,21]. We conclude with that the here presented good agreement between theory and experiments opens experimental avenues to directly obtain τ from tensile strength data.

[1] M.D. Uchic, P.A. Shade, D.M. Dimiduk, Annu. Rev. Mater. Sci. 39 (2009) 361.
[2] J.R. Greer, J.T.M. De Hosson, Prog. Mater. Sci. 56 (2011) 654.
[3] J.A. El-Awady et al., Scr. Mater. 68 (2013) 207.
[4] M.C. Miguel et al., Nature 410 (2001) 667.
[5] R.F. Tinder, J.P. Trzil, Acta Metall. 21 (1973) 975.
[6] D.M. Dimiduk et al., Science 312 (2006) 1188.
[7] M. Zaiser et al., Philos. Mag. 88 (2008) 3861.
[8] R. Maass, P.M. Derlet, J.R. Greer, Small 11 (2015) 341.
[9] R. Maass, P.M. Derlet, J.R. Greer, Scr. Mater. 69 (2013) 586.
[10] M. Zaiser, Adv. Phys. 55 (2006) 185.
[11] P.M. Derlet, R. Maass, Philos. Mag. (2014), http://dx.doi.org/10.1080/14786435.2014.932502.
[12] K.S. Ng, A.H.W. Ngan, Acta Mater. 56 (2008) 1712.
[13] N. Friedman et al., Phys. Rev. Lett. 109 (2012) 095507.
[14] P.D. Ispanovity et al., Acta Mater. 61 (2013) 6234.
[15] A. Rinaldi et al., Acta Mater. 56 (2008) 511.
[16] J.W. Chung, J.T.M. De Hosson, E. van der Giessen, Phys. Rev. B 65 (2002) 094104.
[17] J.W. Chung, J.T.M. De Hosson, Phys. Rev. B 66 (2002) 064206.
[18] J. Senger et al., Acta Mater. 59 (2011) 2937.
[19] P.M. Derlet, R. Maass, Philos. Mag. 93 (2013) 4232.
[20] P.D. Ispanovity et al., Phys. Rev. Lett. 112 (2014) 235501.
[21] S. Papanikolaou et al., Nature 490 (2012) 517.